PNAS
www.pnas.org

Supplementary Information for:

First-in-class, small-molecule allosteric activators of PDE4 long form cyclic AMP phosphodiesterases

Faisa Omar[1], Jane E. Findlay[1], Gemma Carfray[1], Robert W. Allcock[1,3], Zhong Jiang[1,3], Caitlin Moore[1], Amy Muir[1], Morgane Lannoy[4], Bracy A. Fertig[5], Deborah Mai[6], Jonathan P. Day[7], Graeme Bolger[8], George S. Baillie[5], Erik Schwiebert[6], Enno Klussmann[9], Nigel J. Pyne[2], Albert C.M. Ong[4], Keith Bowers[1, 2], Julia M. Adam[1], David R. Adams[1,3], Miles D. Houslay[*,1,10] and David J. P. Henderson[*,1,2]

[1] Mironid Ltd., BioCity Scotland, Bo'ness Road, Newhouse, North Lanarkshire, ML1 5UH, Scotland, UK

[2] Strathclyde Institute of Pharmacy and Biomedical Sciences, University of Strathclyde, 16 Richmond Street, Glasgow, G1 1XQ, Scotland, UK

[3] Institute of Chemical Sciences, Heriot-Watt University, Edinburgh, EH14 4AS, UK

[4] Academic Nephrology Unit, Department of Infection Immunity & Cardiovascular Disease, University of Sheffield Medical School, Beech Hill Road, Sheffield, S10 2RX, UK

[5] Institute of Cardiovascular and Medical Sciences, University of Glasgow, Glasgow G12 8QQ, UK

[6] Discovery Biomed, 400 Riverhill Business Park Suite 435, Birmingham, AL 35424, USA

[7] Department of Genetics, University of Cambridge, Cambridge, UK

[8] Department of Medicine, University of Alabama at Birmingham, Birmingham, AL 35294-3300, USA

[9] Max-Delbrück-Centrum für Molekulare Medizin (MDC), Robert-Rössle-Str. 10, 13092 Berlin, Germany and Charité - Universitätsmedizin Berlin, Corporate Member of Freie Universität Berlin, Humboldt-Universität zu Berlin, and Berlin Institute of Health, Institut für Vegetative Physiologie, Berlin, Germany

[10] School of Cancer and Pharmaceutical Sciences, King's College London, Franklin-Wilkins Building, 150 Stamford Street, London SE1 9NH, UK

Paste corresponding author name here
Email: david.henderson@mironid.com

www.pnas.org/cgi/doi/10.1073/pnas.1822113116

This PDF file includes:

Supplementary Materials and Methods
SI Appendix Figs. S1 to S4

Supplementary Information Text

Additional Materials and Methods

Reverse transcription and qPCR: Reverse transcription of total cellular RNA was conducted using Superscript Vilo reagent (Invitrogen) as per the manufacturer's instruction. Real time qPCR was conducted using an ABI Step-one Plus system and software.

cAMP FRET: Assays were conducted as previously described (1). HEK293 cells were seeded onto sterile glass coverslips and incubated for 24 hours. The cells were transiently transfected with a FRET sensor based on the structure of EPAC1 (EPAC1-cAMPs) using Lipofectamine LTX (Invitrogen). FRET imaging was performed 24 hours following transfection and 40 minutes following pre-incubation with MR-L2. For imaging, the cells were buffered in a solution of 125 mM NaCl, 5 mM KCl, 20 mM HEPES, 1 mM Na_3PO_4, 1 mM $MgSO_4$, 1 mM $CaCl_2$ and 5.5 mM glucose, pH7.4 and stimulated with 1 μM forskolin followed by a saturating concentration of 25 μM forskolin + 100 μM IBMX. Analysis was undertaken using an Olympus IX71 inverted microscope with a 60x oil immersion objective (Zeiss) and an optical beam splitter (Photometrics). MetaFluor software (Molecular Devices) allowed image acquisition and real time monitoring. FRET changes were measured by excitation at 440 nm and obtaining a ratio of the intensity of emissions at 480 nm and 545 nm. Data are expressed as the % FRET change normalized to the baseline FRET ratio at t=0.

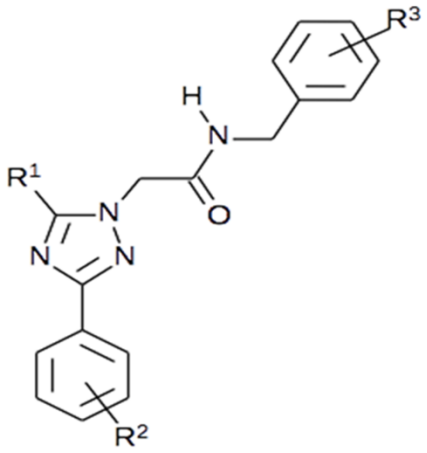

Compound	R^1	R^2	R^3	[μM] = **ECΔ50%**
A	Et	3-F, 4-Cl	3-F	20
B	H	3-F, 4-Cl	3-F	100
C	Me	3-F, 4-Cl	3-F	30
D	CF_3	3-F, 4-Cl	3-F	30
E	CH_2OCH_3	3-F, 4-Cl	3-F	30
F	CH_2OCH_3	4-Cl	3-F	100
G	Et	4-Br	3-F	100
H	Et	4-OCF_3	3-F	20
I	Et	3-F, 4-Cl	H	30
J	Et	3-F, 4-Cl	2-F	20
K	Et	3-F, 4-Cl	4-F	10
L	Et	3-F, 4-Cl	3-Cl	20
M	Et	3-F, 4-Cl	3-CN	30
N	Et	3-F, 4-Cl	3-CF_3	10
O	Et	3-F, 4-Cl	3-0Me	10
P	Et	3-F, 4-Cl	3-OCF_3	10
Q	Et	3-F, 4-Cl	3,5-di-F	30
MR-L2	Et	3-F, 4-Cl	3,5-di-Cl	10

Fig. S1. MR-L2 is listed alongside representative examples from the substituted triazole activator compound series (Additional compounds are listed as A-Q). Concentrations at which the pharmacological activation of human long form PDE4D5 reached 50% are shown. Three regions around the central core of the novel activator chemotype were explored for initial SAR development: R1, the triazole 5-substituent; R2, the pendant aromatic ring substitution and R3, the benzyl amide side chain substitution.

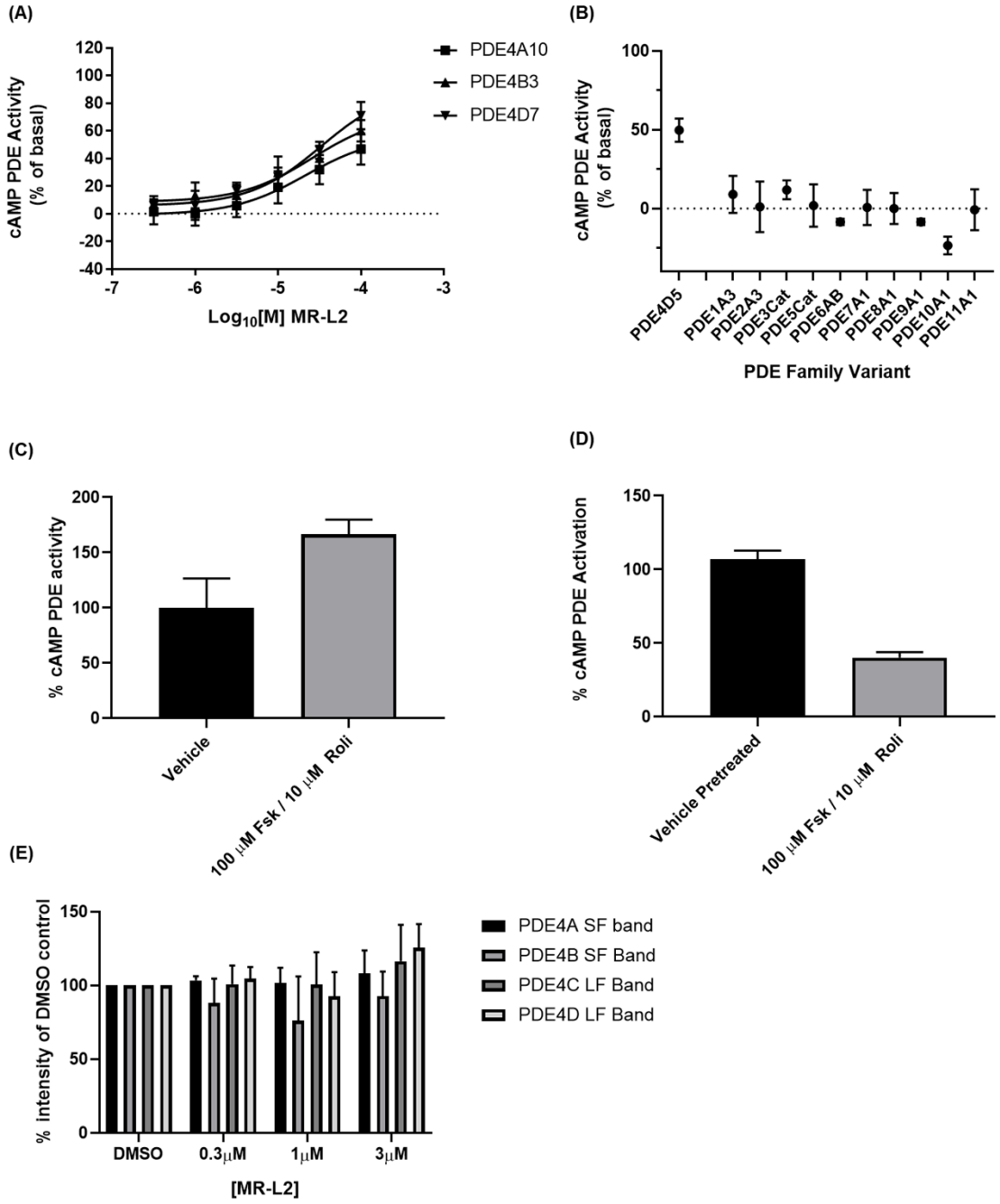

Fig. S2. (A) MR-L2 activates additional long-form PDE4 enzymes from PDE4A, PDE4B and PDE4D enzyme families. Error bars represent SD of at least 3 independent experiments. (B) No significant activation was observed in response to the treatment in other catalytically active PDE family species treated with 30 μM MR-L2. (C) It is possible to drive PKA phosphorylation of long PDE4 isoforms by chronically elevating intracellular cAMP levels through treating cells with forskolin (a direct activator of adenylyl cyclase in the presence of pharmacological PDE inhibitors, to attenuate cAMP degradation, prior to cell lysis and assay. The entire complement of PDE4 long-long isoforms is unlikely to be phosphorylated in such circumstances as phosphorylated PDE4 long isoforms will be subject to dynamic, phosphatase-driven dephosphorylation at the same time and a steady state will be reached. However, in support of the observation that the PKA mediated phosphorylation and activation of PDE4 long isoforms is

not additive, and that the pharmacological activation of PDE4 long isoforms mirrors activation by PKA phosphorylation, we additionally show that forskolin/rolipram pre-treatment enhances PDE4D5 lysate cAMP PDE activity and (D) reduces maximal pharmacological activation by ~60% in harvested lysates expressing PDE4D5. No significant change was observed in the protein expression of PDE4 isoform variants. Densitometry was conducted on films derived of three experiments, where the error bars represent the standard deviation. SF = Short form, LF = long form.

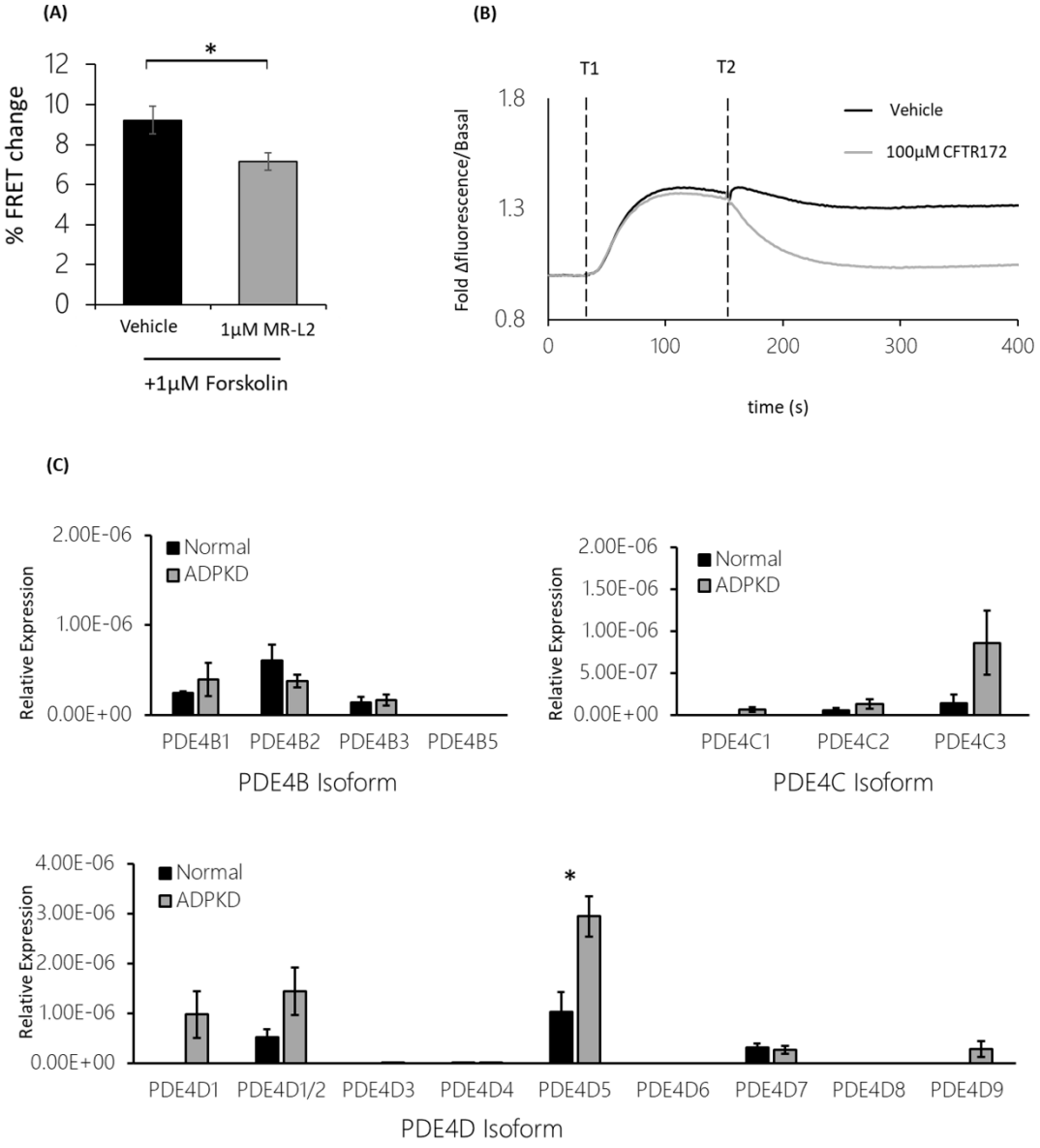

Fig. S3. (A) cAMP responsive FRET change in response to 1 μM forskolin stimulation. Preincubation with 1 μM of MR-L2 is sufficient to reduce cAMP-induced FRET ($p<0.05$) indicating a suppression of cAMP. (B) Membrane depolarization induced by 100 nM PGE2 (T1) is reversed by the addition of the CFTR inhibitor CFTR172 (100 μM, T2). (C) The expression of PDE4 isoform variants was assessed by qPCR targeted toward the unique N-terminal region of PDE4 isoform variants. Total RNA from 4 normal and 4 ADPKD cell lines were probed, and gene expression values are displayed relative to 18s rRNA abundance. Error bars represent the standard error of the mean between samples.

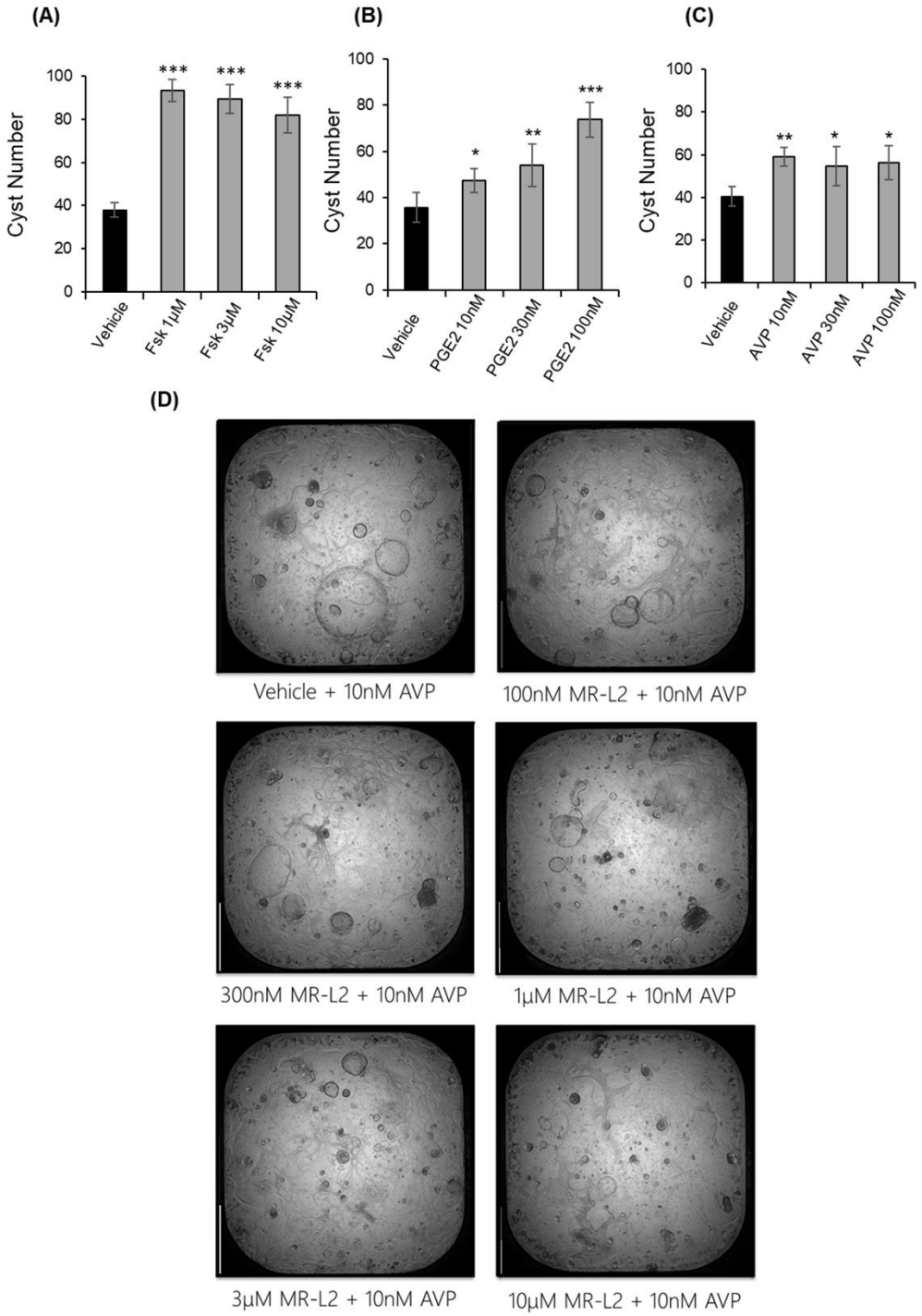

Fig. S4. (A) Primary human kidney epithelial cells from an ADPKD patient form cysts in 3D culture. Stimulation with forskolin enhances cystogenesis. (B) Stimulation with the Gs GPCR agonists PGE2 and (C) Vasopressin also enhance cystogenesis. (D) Representative images of MR-L2 treated cells grown in 3D culture and stimulated with 10 nM vasopressin.

SI Appendix References

1. Sin YY, *et al.* (2011) Disruption of the cyclic AMP phosphodiesterase-4 (PDE4)-HSP20 complex attenuates the beta-agonist induced hypertrophic response in cardiac myocytes. *J Mol Cell Cardiol* 50(5):872-883.